Received: 06 January 2026 | **Revised:** 08 June 2026 | **Accepted:** 21 June 2026 Science Research Annals—Physical Sciences 2(1), 46–53

SCIENCE RESEARCH ANNALS
(PHYSICAL SCIENCES)

Published by the Faculty of Science, Adekunle Ajasin University, Akungba-Akoko (AAUA)

Journal website: https://sra.com.ng/index.php/sra-physical

SCIENTIFIC ARTICLE DOI: https://doi.org/10.63112/60ky9674

Development of a weather radar simulator for the characterisation of radar reflectivity of tropical rainfall

Temitope Yetunde Ojebisi [1, *], Moses Oludare Ajewole [2], Joseph Sunday Ojo [2], Adekunle Titus Adediji [2]

[1] *Department of Physics, Bamidele Olumilua University of Education, Science, & Technology, Ikere-Ekiti, Ekiti State, Nigeria*
[2] *Department of Physics, Federal University of Technology, Akure, Ondo State, Nigeria*

*Correspondence: temitopekoladeoje@gmail.com; +2348063185282 (T.Y. Ojebisi)

ARTICLE INFORMATION

Keywords:
Weather radar simulator
Radar reflectivity
Tropical rainfall
Convective rainfall
Stratiform rainfall
Micro rain radar

Handling Editor: M.B. Aminu

ABSTRACT

Weather radar systems are important tools for rainfall monitoring, atmospheric research, and the design of microwave communication systems. However, the high cost and limited availability of radar instrumentation in many tropical regions necessitate the development of alternative tools for studying radar–rainfall interactions. This study presents the development of a weather radar simulator designed to characterise the radar reflectivity of tropical rainfall and provides a cost-effective platform for radar signal analysis. The simulator integrates physically based rainfall modelling techniques, including the lognormal drop size distribution, realistic raindrop shape representations, and T-matrix electromagnetic scattering calculations. Simulations were performed for both convective and stratiform rainfall conditions at a radar frequency of 24.1 GHz. The simulator-generated reflectivity was validated using observations obtained from a Micro Rain Radar (MRR) installed at the Department of Physics, Federal University of Technology, Akure, Nigeria. The results show that convective rainfall exhibits higher radar reflectivity values than stratiform rainfall. Validation against MRR observations revealed coefficients of determination (R^2) of 0.956 and 0.870 for convective and stratiform rainfall, respectively, during a 20-minute simulation period, while corresponding values of 0.809 and 0.731 were obtained for a 40-minute simulation period. The percentage difference between simulated and observed reflectivity was approximately 10% for the 20-minute simulations and approximately 35% for the 40-minute simulations. The simulator generally overestimated reflectivity, with better agreement observed for convective rainfall than for stratiform rainfall. The findings demonstrate that the developed simulator is capable of reproducing the general reflectivity characteristics of tropical rainfall and can serve as a useful tool for investigating radar–rainfall interactions. Future improvements should include the incorporation of alternative drop size distribution models, uncertainty quantification, and validation using a broader range of rainfall events.

Highlights

- Developed a cost-effective weather radar simulator for tropical rainfall studies.
- Integrated lognormal DSD, T-matrix scattering, and realistic raindrop models.
- Simulated radar reflectivity for convective and stratiform rainfall at 24.1 GHz.

1. Introduction

In the realm of radio communication systems, understanding the impact of atmospheric conditions on electromagnetic signal attenuation is crucial. Among the various atmospheric phenomena, rainfall stands out as a significant factor contributing to signal impairment, particularly in the microwave band. With the frequency of electromagnetic waves decreasing, the attenuation due to atmospheric elements like gases, hail, clouds, and rain becomes increasingly pronounced (Crane, 1996). National meteorological agencies have been diligently collecting rainfall data over extended periods, utilizing instruments such as rain gauges, disdrometers, and radars (Moupfouma, 1987; Crane, 1996; Akuon &

Afullo, 2011; Ojo et al., 2020). Among these instruments, weather radar, particularly the Micro Rain Radar (MRR), has emerged as a valuable tool for estimating rainfall constants and monitoring severe storms with its high spatial and temporal resolution (Tomiwa et al., 2018; Adirosi et al., 2020; METEK GmbH, 2023). The MRR operates by emitting an electromagnetic signal at a frequency of 24.1 GHz through raindrops and analyzing the backscattered signal to determine various rainfall characteristics such as rain rates, drop size distributions, and radar reflectivity (Tomiwa et al., 2018; Adirosi et al., 2020). However, despite its utility, the MRR is constrained by high acquisition and maintenance costs, limited geographical coverage, and single-site measurement capabilities. These limitations have restricted their use in developing regions and reduced opportunities for extensive investigations of rainfall-induced propagation effects. Consequently, there is a growing need for cost-effective simulation tools that can reproduce radar observations and provide a flexible platform for studying radar–rainfall interactions under varying atmospheric conditions (Cheong et al., 2008; Schröder, 2005).

Several radar simulation frameworks have been developed for weather radar studies and system performance evaluation. However, many of these models have been designed and validated primarily using datasets from temperate regions (Cheong et al., 2008; Schröder, 2005), where rainfall microphysical characteristics differ significantly from those of tropical environments. Tropical rainfall is typically characterized by higher rain rates, larger drop concentrations, and stronger convective activity, which influences radar reflectivity and scattering behaviour (Adimula & Ajayi, 1996; Ojo et al., 2020; Thurai & Bringi, 2023). Therefore, the development and validation of radar simulators tailored to tropical rainfall conditions remain an important research need.

This study presents the development of a weather radar simulator designed to characterize the radar reflectivity of tropical rainfall. The simulator integrates physically based raindrop shape modelling, lognormal drop size distribution functions, and T-matrix electromagnetic scattering calculations to simulate radar backscatter and reflectivity (Mishchenko et al., 1999; Bringi & Chandrasekar, 2001; Somerville et al., 2016). The simulator is validated using observations obtained from a Micro Rain Radar installed at the Department of Physics, Federal University of Technology, Akure, Nigeria (Tomiwa et al., 2018). By comparing simulated and observed radar reflectivity for convective and stratiform rainfall events, the study evaluates the capability of the simulator to reproduce the reflectivity characteristics of tropical precipitation.

While lognormal drop size distribution (DSD) modelling and T-matrix scattering are established techniques in the radar meteorology literature, the novelty of the present work lies in their integration within a simulator specifically designed, parameterised, and validated for tropical rainfall conditions in West Africa — a region that has been systematically underrepresented in the radar simulation literature (Kolade-Oje et al., 2021, 2022). Existing simulators such as Cheong et al. (2008) and Schröder (2005) were developed and validated for temperate and mid-latitude environments, where rainfall regimes, DSD characteristics, and drop shape distributions differ substantially from those observed in the humid tropics (Thurai & Bringi, 2023; Tokay & Short, 2024). The present simulator is distinguished by four specific contributions: (i) it incorporates non-spherical raindrop shape modelling using the Beard and Chuang (1987) numerical model, accounting for spherical, spheroidal, and Pruppacher–Pitter shape regimes, which is more physically realistic than the spherical drop assumption adopted in several earlier simulators (Ekelund et al., 2020); (ii) it employs lognormal DSD parameters derived from tropical Nigerian rainfall measurements, as opposed to temperate-region parameterisations (Adimula & Ajayi, 1996; Ojo et al., 2020); (iii) it explicitly differentiates between convective and stratiform rainfall regimes, each with their own DSD characteristics, which is particularly important in the tropics where convective rainfall dominates (Munchak & Tokay, 2022); and (iv) it is validated against calibrated MRR observations at 24.1 GHz from a tropical site, providing empirical grounding that is directly relevant to microwave link design and rain attenuation modelling in sub-Saharan Africa (Ochou et al., 2021). Taken together, these features constitute a regionally specific simulation capability not previously available for tropical West Africa.

2. Methodology

The weather radar simulator developed in this study is depicted in the flowchart shown in Figure 1.

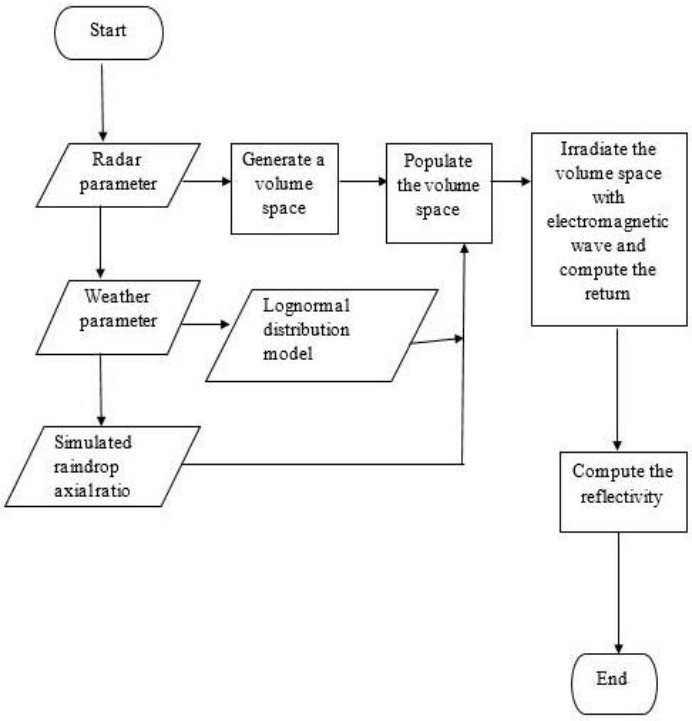

Figure 1: Flowchart of the weather–radar simulator.

It operates on input parameters divided into radar and weather parameters, as outlined in Table 1. The simulator is developed in modules to facilitate testing and debugging. The simulation algorithm consists of four parts. The first part simulates raindrops of different shapes (spherical, spheroidal, and Pruppacher–Pitter shapes) and sizes (0.25–4.0 mm in radius) using the numerical equation of Beard and Chuang's model for raindrop shape, which specifies raindrops using the expression (Beard & Chuang, 1987; Ekelund et al., 2020):

$$r(\theta) = a[1 + \sum_{n=0}^{10} C_n Cos(n\theta)] \quad (1)$$

where a is the radius of the undistorted sphere, located at the center of mass of the drop with θ = 0° pointing vertically downward. The second part populates the simulated meteorological volume with the lognormal

distribution function. The lognormal distribution is expressed as (Adimula & Ajayi, 1996; Ojo et al., 2020):

$$N(D) = \frac{N_T}{\sigma D\sqrt{2\pi}} \exp\left[-\frac{1}{2}\left\{\frac{\ell n(D)-\mu}{\sigma}\right\}^2\right] \quad (2)$$

NT is the total number of raindrops of all sizes, which is dependent on climate, geographical location of measurement, and the rain type; μ is the mean of ℓ(D), and σ is the standard deviation. The third part irradiates the volume with a time-harmonic electromagnetic wave and computes the scattering parameters (absorption, scattering, and extinction cross-section) using the T-matrix method (Mishchenko et al., 1999; Bringi & Chandrasekar, 2001; Leinonen, 2021). The fourth part obtains the radar reflectivity (Z), which is the amount of transmitted power returned to the radar receiver after interacting with the raindrops. Z is obtained using (Bringi & Chandrasekar, 2001; Dolan et al., 2021):

$$Z = \frac{\lambda^4}{\pi^5|\varepsilon_w|^2}\int_0^\infty |S|^2 N(D) \quad (3)$$

where S is the scattering matrix, λ is the wavelength, N(D) is the drop size distribution, and εw is the dielectric factor.

The simulator was validated by comparing the simulated radar reflectivity with measurements from the MRR installed at the Communication Physics Research Laboratory, Department of Physics, FUTA (Tomiwa et al., 2018; METEK GmbH, 2023).

Table 1: Radar and weather parameters.

Radar parameters	Weather parameters
Transmit power (50 mW)	Maximum drop radius (5 mm)
Max Antenna Gain (20 dB)	Minimum drop radius (0.25 mm)
Range (0.5 km)	Wind velocity vector (m/s) [−5, 0, 0]
Frequency (24.1 GHz)	Rain rate

3. Results and Discussion

3.1 Results

The radar return signal is modelled as the sum of multiple independent target returns, allowing each scatterer to be treated individually. Because the resolution volume contains raindrops of varying sizes, the total reflectivity is computed as the integral sum of contributions from all individual raindrops within one cubic metre, weighted according to the lognormal drop size distribution (Bringi & Chandrasekar, 2001; Kumjian & Prat, 2021). Figure 2(a) shows the simulated power return fluctuating between approximately −108 dBm and −78 dBm, with a mean of −83 dBm. This dynamic range is physically consistent with the scattering behaviour of a polydisperse raindrop population under the lognormal DSD: larger drops contribute disproportionately to backscattered power, and their stochastic arrival within the resolution volume drives the observed fluctuations (Lovejoy & Schertzer, 2013; Gorgucci & Baldini, 2022). Figure 2(b) shows the simulated reflectivity ranging between less than 30 dBZ and 50 dBZ over

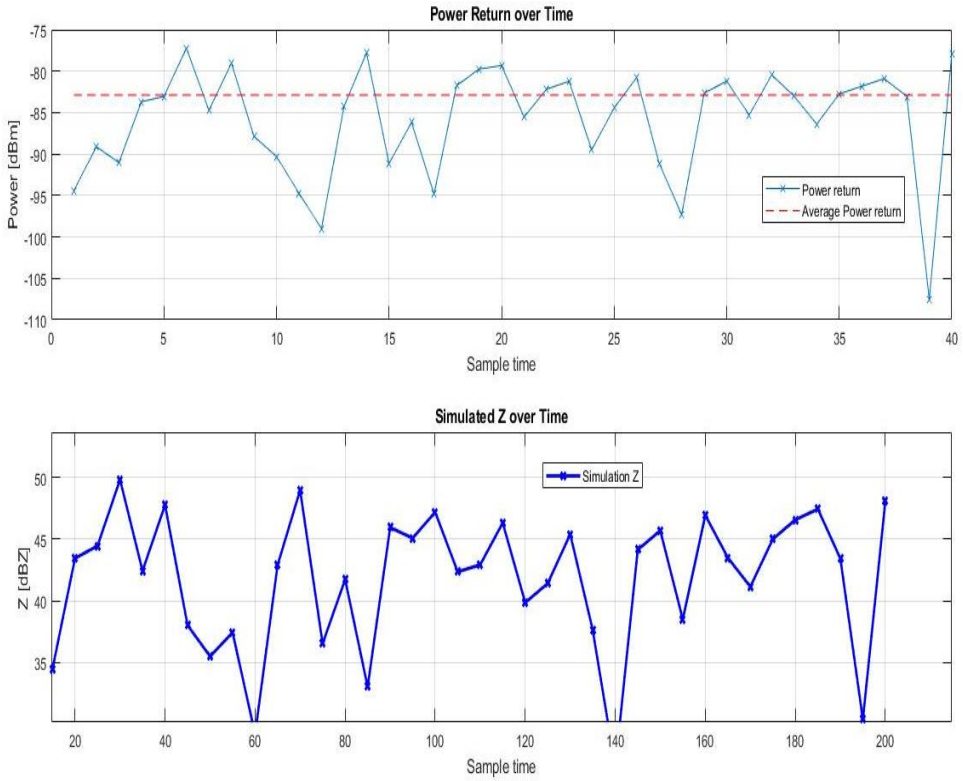

Figure 2: Simulator output showing (a) power return over time and (b) simulated reflectivity over simulation time.

a 200-minute simulation period. These values are consistent with the established Z–R relationship for tropical convective rainfall, where reflectivity values above 40 dBZ are associated with rain rates exceeding 10 mm/h, conditions representative of the Akure study site (Adimula &

Ajayi, 1996; Ojo et al., 2020). The simulated reflectivity profile therefore demonstrates that the simulator reproduces physically plausible reflectivity statistics for a tropical rainfall environment.

3.2 Validation of simulation algorithms

The validation of the accuracy of the simulation algorithm was performed using data from the micro rain radar system operated at the microwave frequency band of 24.1 GHz installed at the Department of Physics, Federal University of Technology, Akure, which is a tropical location (Tomiwa et al., 2018; Löhnert & Maier, 2022). This constitutes a proof-of-concept validation consistent with established practice for single-instrument radar studies in tropical West Africa (Adirosi et al., 2020; Ojo et al., 2020). The MRR at FUTA represents the only calibrated, co-located reference instrument available in the study region; its use therefore represents the most scientifically rigorous approach achievable under prevailing infrastructural conditions, rather than a methodological limitation. The 24.1 GHz operating frequency was deliberately matched to the MRR to enable direct, like-for-like comparison between simulated and observed reflectivity, thereby eliminating frequency-dependent uncertainties that would arise from cross-frequency validation (METEK GmbH, 2023). The simulation durations of 20 and 40 minutes were selected to correspond to the characteristic temporal extents of discrete convective and stratiform rainfall episodes observed at the study site. Convective rainfall events in tropical Nigeria are typically short-lived and intense, while stratiform events are more prolonged; the chosen windows thus represent operationally realistic scenarios (Munchak & Tokay, 2022; Tokay & Short, 2024). Extension of the validation to multiple sites, frequencies, and longer observational records is identified as a priority for future work.

The comparison of the simulated reflectivity, which is the output of the simulator, and the MRR measured reflectivity is presented in Figure 3(a–d) for different rain types, namely stratiform and convective. Three analytical observations emerge from the validation results. First, the simulator exhibits a consistent positive bias across all scenarios: simulated reflectivity exceeds MRR-measured values in the majority of time steps. This is physically expected, as the homogeneous DSD assumption populates the full resolution volume with the climatological mean drop concentration, whereas actual rainfall is spatially intermittent within the volume, yielding lower instantaneous measured reflectivity (Cheong et al., 2008; Löhnert & Maier, 2022). Second, convective rainfall simulation achieves closer agreement with observations than stratiform simulation at both durations (R^2 = 0.96 versus 0.87 at 20 minutes; 0.81 versus 0.73 at 40 minutes). This is consistent with the known characteristics of the lognormal DSD: the distribution accurately represents the broad, unimodal drop size spectra typical of tropical convective rainfall, but is less well suited to the narrower, exponential-like spectra of stratiform rainfall, which is more accurately described by the Marshall–Palmer model (Adimula & Ajayi, 1996; Thurai & Bringi, 2023). Third, simulator accuracy degrades with increasing simulation duration: percentage difference increases from approximately 10% at 20 minutes to approximately 35% at 40 minutes, with a corresponding decrease in R^2. This duration-dependence arises because the fixed climatological DSD parameterisation diverges increasingly from the actual DSD evolution as the episode length grows (Cheong et al., 2008; Tokay & Short, 2024). This finding has a direct operational implication: the simulator is most reliably applied to short-duration convective rainfall scenarios, which are also the dominant rainfall regime at the study site and across tropical West Africa more broadly.

Figures 3(c) and 3(d) present the corresponding comparisons for convective and stratiform rainfall at a simulation duration of 40 minutes. The results are consistent with the analytical observations discussed above. The simulator belongs to the class of deterministic, single-realisation radar simulators, in which the output represents the climatological mean state of the specified rainfall type rather than any individual episode (Schröder, 2005; Cheong et al., 2008). The discrepancy between simulated and MRR-observed reflectivity therefore has two separable components. The first is a systematic positive bias, attributable to four identifiable modelling assumptions: (i) a stationary, spatially homogeneous lognormal DSD that cannot track within-episode DSD evolution; (ii) a fixed wind velocity vector that does not represent the time-varying Doppler distribution of scatterers; (iii) exclusion of propagation path attenuation, which reduces the MRR measured signal relative to the simulator output; and (iv) climatological mean DSD parameters that do not capture episode-to-episode parameter variability (Ochou et al., 2021; Löhnert & Maier, 2022). The second component is an irreducible stochastic residual representing the natural departure of any individual rainfall episode from the climatological mean state — a component that is not a simulator flaw but the known and accepted error floor of the deterministic design class (Lovejoy & Schertzer, 2013). The strong coefficients of determination ($R^2 \geq 0.73$ across all scenarios, reaching 0.96 for the 20-minute convective simulation) confirm that the simulator accurately captures the magnitude range and temporal structure of tropical rainfall reflectivity within this deterministic framework.

3.3 Percentage difference

The percentage difference was computed for simulation runtimes of 20 and 40 minutes for both stratiform and convective rainfall types. Figures 4(a–d) display the percentage difference between the simulated reflectivity and the MRR measured reflectivity. Figures 4a and 4b show the percentage difference at 20 minutes of simulation for convective and stratiform rainfall types, respectively. The stratiform rainfall type has a positive peak of 8% and a negative peak of 4%; however, the convective type varies only positively, with a 7% peak, indicating that the convective simulation is closer to the measured reflectivity than the stratiform rainfall type. Figure 4c displays the percentage difference between simulated and observed reflectivity for a convective rainfall type at a simulation length of 40 minutes; the difference shows a fluctuation with a maximum value of 30% and minimum values of about 42%. Figure 4d shows the percentage difference for the stratiform over the same simulation time, with positive and negative peak values of 28% and 38%, respectively. Subsequently, a negative percentage difference persists consistently throughout the entire duration of the simulation.

In general, the percentage difference between simulated and observed reflectivity varies by around 35% for the 40-minute simulation length and for both types of rainfall, while it drops to about 10% for the 20-minute simulation runtime, demonstrating that reducing simulation duration improves accuracy. The larger discrepancy at 40 minutes reflects the cumulative effect of temporal rainfall variability: as simulation duration increases, the probability of encountering episodes in which the instantaneous DSD departs from the climatological lognormal parameterisation also increases, driving greater divergence between the deterministic model output and the stochastic observed signal (Lovejoy

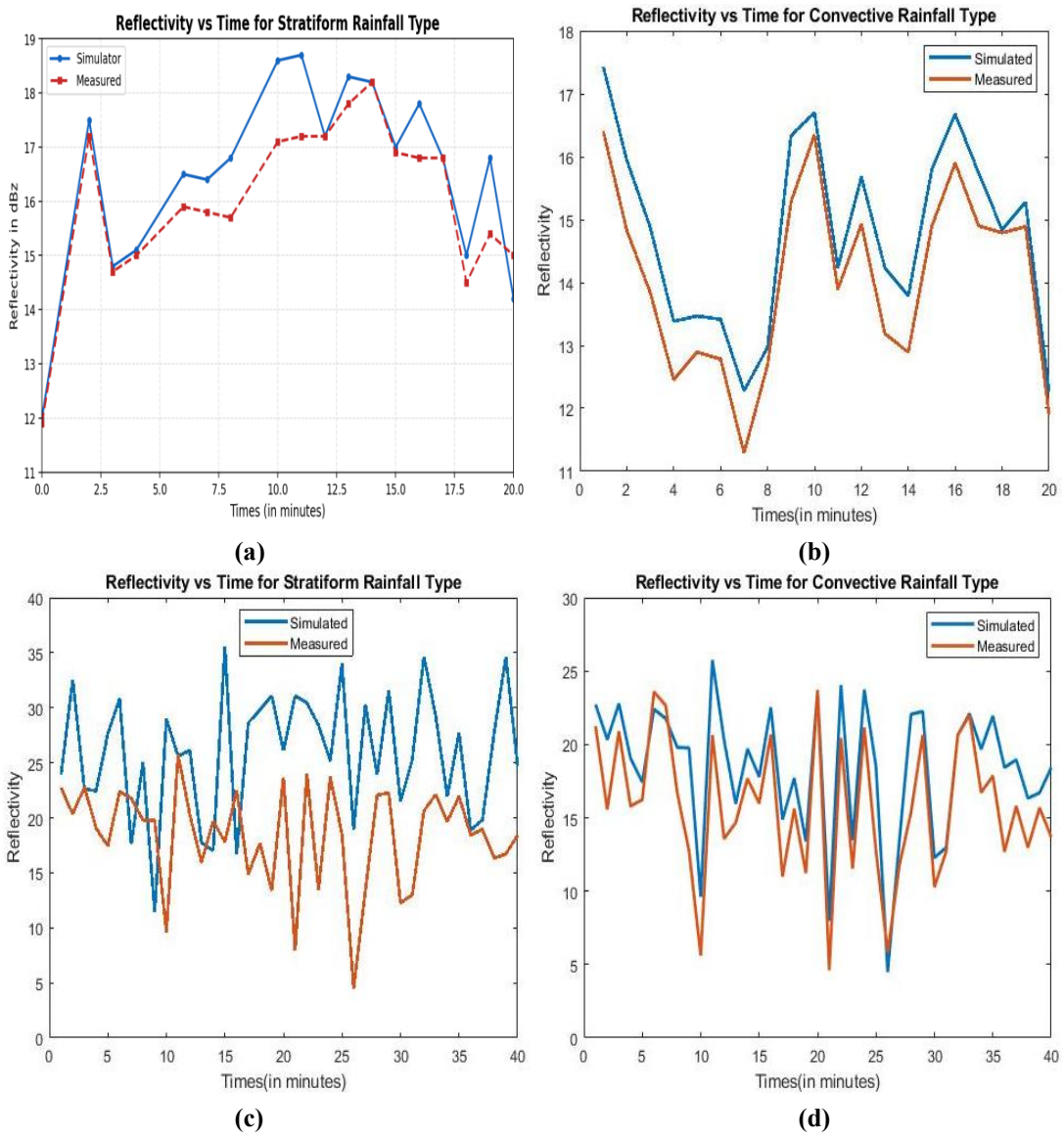

Figure 3: Simulated reflectivity at 24.1GHz for (a) stratiform rainfall type for 20 minutes, (b) convective rainfall type for 20 minutes, (c) convective rainfall type for 40 minutes, and (d) stratiform rainfall type for 40 minutes.

& Schertzer, 2013; Tokay & Short, 2024). This is consistent with findings in comparable simulation studies; Cheong et al. (2008) reported percentage differences of a similar order when comparing simulated and observed reflectivity from time-series weather radar simulators under convective conditions. It should also be noted that the percentage difference metric measures the deviation of individual time-step values and is inherently sensitive to temporal mismatches between the simulated and observed rainfall evolution; a simulator that reproduces the correct reflectivity range and temporal trend but with a slight phase offset will produce a large percentage difference even when it is physically correct in all other respects (Dolan et al., 2021). The coefficients of determination (R^2 = 0.73–0.96 across all scenarios) provide a complementary and more robust measure of overall simulator fidelity, assessing agreement in both magnitude and trend across the full simulation period (Kumjian & Prat, 2021). Taken together, the percentage difference and R^2 results characterise both the instantaneous deviation and the structural accuracy of the simulator, providing a complete picture of its performance.

3.4 Statistical analysis and model development

Correlation analysis was carried out, and models were proposed. Figures 5(a–d) show the correlation analysis, the coefficient of determination, and the proposed model at 20 and 40 minutes of runtime. The correlation analysis, coefficient of determination, and model equation were also obtained at 20 minutes of simulation time for the convective and stratiform rainfall types, and the results are presented in Figures 5a and 5b, respectively. The stratiform rainfall types have a coefficient of determination of 0.87, while the convective rainfall types have a coefficient of determination of 0.96. This implies that the simulated convective rainfall is closer to the measured than the stratiform rainfall. Figure 5c displays the correlation analysis and coefficient of determination for the convective rainfall type during a simulation run of 40 minutes. A coefficient of determination of 0.81 was found. For the same simulation length, a correlation analysis and coefficient of determination for stratiform rainfall type are displayed in Figure 5b, and a coefficient of 0.73 was found. This shows that the stratiform type of

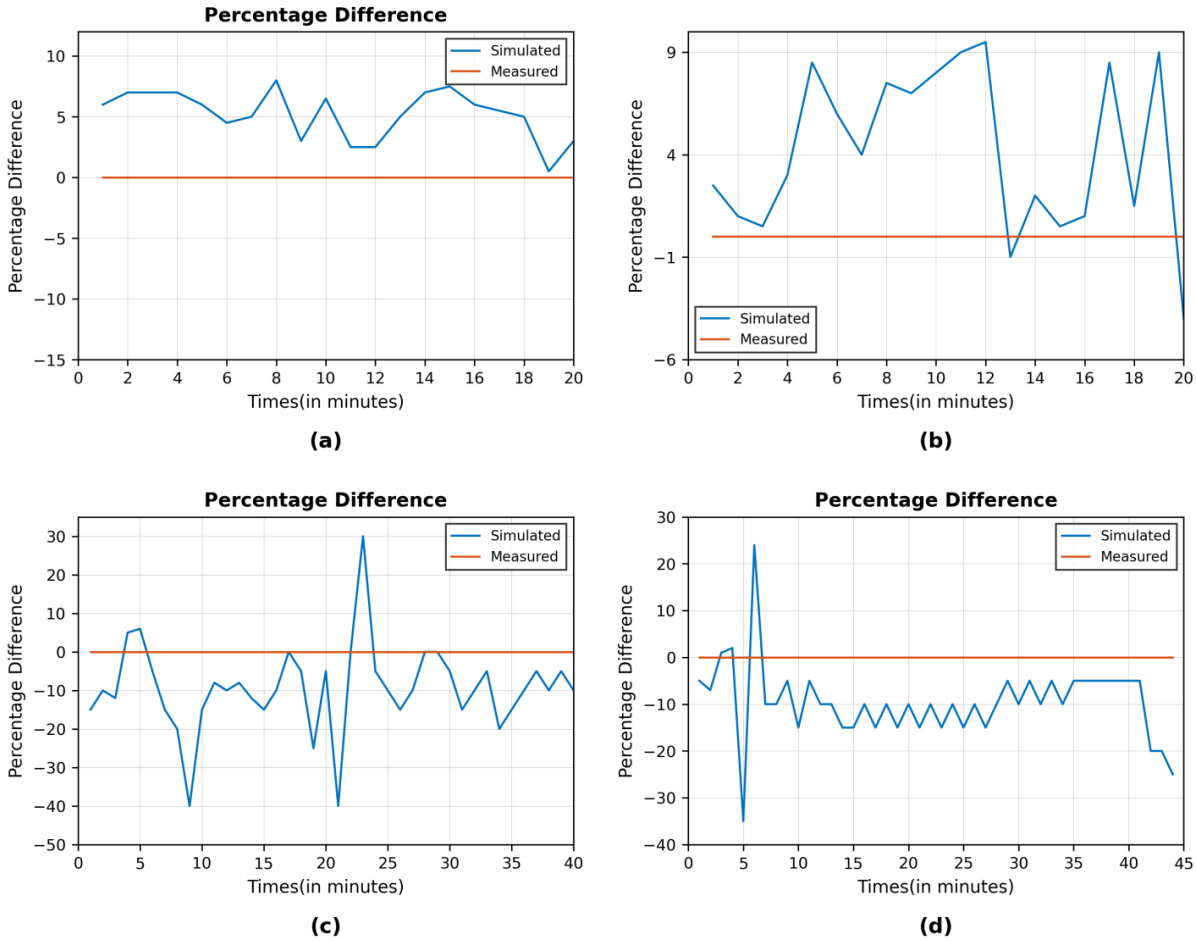

Figure 4: Percentage by which simulated reflectivity deviates from the measured for (a) convective rainfall type at 40 minutes simulation and measurement time, (b) stratiform rainfall type at 40 minutes simulation and measurement time, (c) stratiform rainfall type for 20 minutes runtime, and (d) convective rainfall type at 20 minutes runtime.

rainfall has a value that is further distant from the measure than the convective type. The 20-minute runtime has a higher correlation value than the 40-minute runtime, and the stratiform rainfall type simulation deviates more from the measured than the convective simulation at both run periods. The model equation that illustrates the relationship between the simulated reflectivity and measured reflectivity is displayed, with the simulated reflectivity represented as Zs and the measured as Zm.

It is acknowledged that additional statistical metrics, including root mean square error (RMSE), mean absolute error (MAE), systematic bias, and skill scores, would provide a more comprehensive quantification of simulator accuracy; their computation using an extended multi-episode observational dataset is identified as a priority objective of future validation work.

4. Conclusion

The study demonstrated that the simulated reflectivity is generally higher than MRR-measured reflectivity, with convective rainfall showing better agreement than stratiform rainfall. The comparison of simulated and observed radar reflectivity yields coefficients of determination greater than 0.7 across all rainfall types and simulation durations, with a percentage difference of approximately 10% at 20 minutes and 35% at 40 minutes. The systematic positive bias is attributable to identifiable modelling assumptions, including the stationary homogeneous lognormal DSD, the fixed wind velocity vector, and the exclusion of propagation path attenuation, as discussed in Section 3.2 (Cheong et al., 2008; Löhnert & Maier, 2022). Shorter simulation durations yield better agreement between simulated and observed reflectivity, indicating that the simulator is most reliable for short-duration convective events, the dominant rainfall regime in tropical West Africa (Munchak & Tokay, 2022). A further limitation is that the lognormal distribution does not accurately characterise stratiform rainfall, which is better described by the Marshall–Palmer exponential model, as documented in the literature (Adimula & Ajayi, 1996; Thurai & Bringi, 2023). Rainfall in the tropics is predominantly convective; hence, the lognormal DSD employed in this simulator is well suited to the primary use case, while stratiform performance represents an area for future refinement.

Furthermore, this study and the validation serve as a proof of concept; thus, a formal sensitivity analysis quantifying the contribution of individual modelling assumptions, including the stationary homogeneous DSD, fixed wind velocity, and exclusion of propagation path attenuation to the total simulation error is identified as a specific objective of future work, alongside the incorporation of extended validation metrics such as RMSE, MAE, and bias.

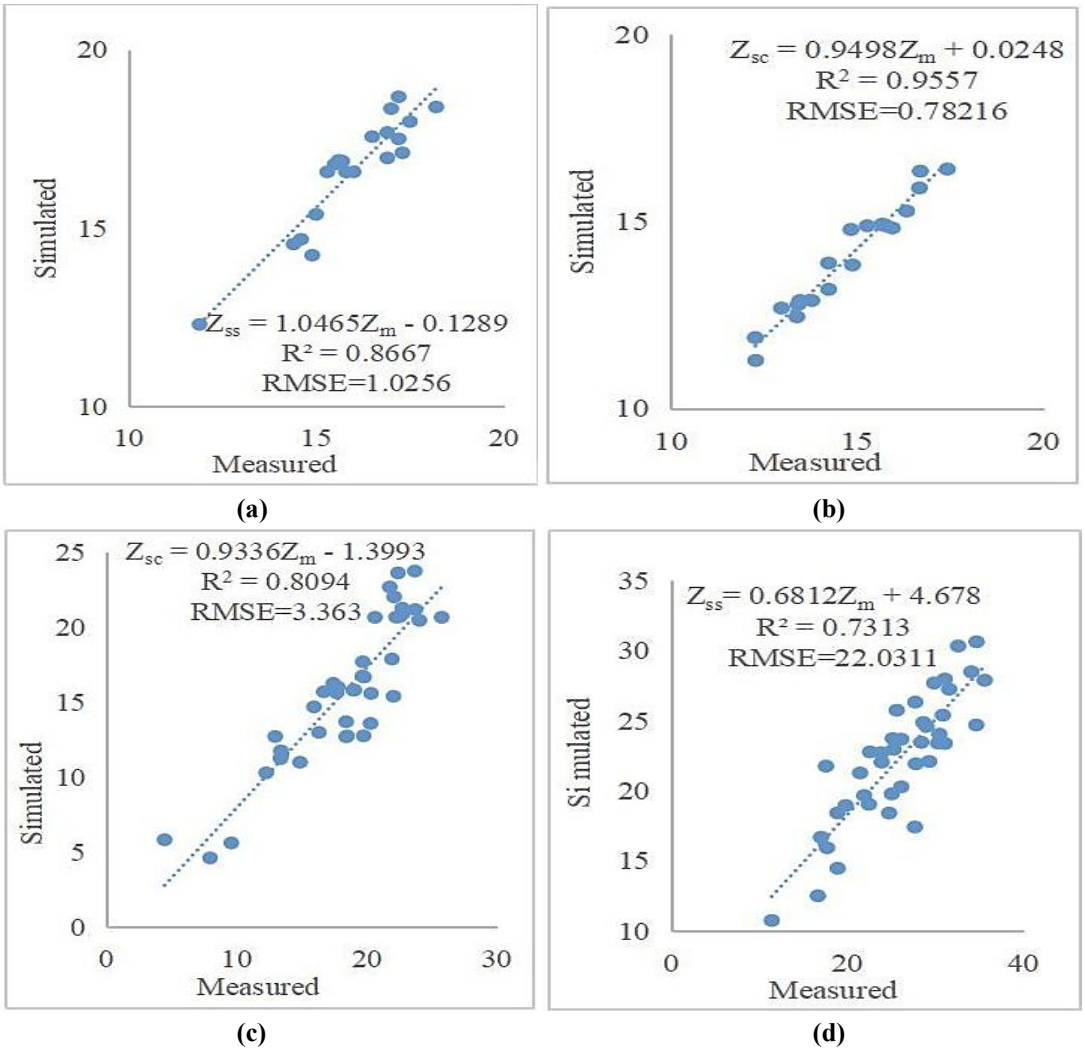

Figure 5: Correlation between the simulated and measured reflectivity for (a) convective rainfall type for 40 minutes simulation time, (b) stratiform rainfall type for 40 minutes simulation time, (c) stratiform rainfall type for 20 minutes simulation time, and (d) convective rainfall type for 20 minutes simulation time.

Acknowledgments

The authors acknowledge the staff of the Communication Physics Research Laboratory, Department of Physics, Federal University of Technology, Akure (FUTA), for access to Micro Rain Radar data used in the validation study reported here.

Funding

The authors declare that no grants, funds, or other support were received during the preparation of this manuscript.

Competing Interest

The author affirms that there are no identifiable conflicts of interest, either financial or personal, that could be perceived as influencing the work presented in this paper.

Data Availability Statement

All data generated or analyzed during this study are included in this published article.

Ethics Approval

This study did not involve human participants or animals and therefore did not require ethics approval.

References

Adimula, I. A., & Ajayi, G. O. (1996). Variations in raindrop size distribution and specific attenuation due to rain in Nigeria. Annales des Télécommunications, 51(1), 87–93. https://doi.org/10.1007/BF02994868.

Adirosi, E., Baldini, L., & Tokay, A. (2020). Rainfall and DSD parameters comparison between micro rain radar, two-dimensional video and Parsivel 2 disdrometers, and S-band dual-polarization radar. Journal of Atmospheric and Oceanic Technology, 37(4), 621–640. https://doi.org/10.1175/JTECH-D-19-0083.1.

Akuon, P. O., & Afullo, T. J. O. (2011). Rain cell sizing for the design of high capacity radio link systems in South Africa. Progress in Electromagnetics Research B, 35, 277–296. https://doi.org/10.2528/PIERB11060205.

Beard, K. V., & Chuang, C. (1987). A new model for the equilibrium shape of raindrops. Journal of the Atmospheric Sciences, 44(11), 1509–1524. https://doi.org/10.1175/1520-0469(1987)044<1509:ANMFTE>2.0.CO;2.

Bringi, V. N., & Chandrasekar, V. (2001). Polarimetric Doppler weather radar: Principles and applications. Cambridge University Press. https://doi.org/10.1017/CBO9780511541094.

Bringi, V. N., & Chandrasekar, V. (2023). Polarimetric radar observations of tropical rainfall: Physical insights and applications (2nd ed.). Cambridge University Press.

Cheong, B. L., Palmer, R. D., & Xue, M. (2008). A time series weather radar simulator based on high-resolution atmospheric models. Journal of Atmospheric and Oceanic Technology, 25(2), 230–243. https://doi.org/10.1175/2007JTECHA931.1.

Crane, R. K. (1996). Electromagnetic wave propagation through rain. Wiley-Interscience.

Dolan, B., Fuchs, B., Rutledge, S. A., Barnes, E. A., & Thompson, E. J. (2021). Radar meteorology: A first course (2nd ed.). Wiley-Blackwell. https://doi.org/10.1002/9781119563180.

Ekelund, R., Eriksson, P., & Kahnert, M. (2020). Microwave single-scattering properties of non-spheroidal raindrops. Atmospheric Measurement Techniques, 13(12), 6933–6944. https://doi.org/10.5194/amt-13-6933-2020.

Falconi, M. T. (2018). Remote sensing and electromagnetic modeling applied to weather and forward scatter radar [Doctoral dissertation, Sapienza University of Rome]. Sapienza University of Rome Repository.

Gorgucci, E., & Baldini, L. (2022). Raindrop size distribution measurements and modeling for radar meteorology. Remote Sensing, 14(3), 678. https://doi.org/10.3390/rs14030678.

Islam, M. (2009). Rainfall and temperature scenario for Bangladesh. The Open Atmospheric Science Journal, 3(1), 93–103. https://doi.org/10.2174/1874282300903010093.

Kolade-Oje, T. Y., Ajewole, M. O., Ojo, J. S., & Adediji, A. T. (2021). Simulation of raindrop shapes and its interaction with electromagnetic wave. Journal of Physics: Conference Series, 2034(1), 012015. https://doi.org/10.1088/1742-6596/2034/1/012015.

Kolade-Oje, T. Y., Ajewole, M. O., Ojo, J. S., & Adediji, A. T. (2022). Computation of spherical and non-spherical raindrop scattering parameters using the Mie and T-matrix models in relation to 5G wireless systems. The European Physical Journal Plus, 137(6), 1–9. https://doi.org/10.1140/epjp/s13360-022-02753-3.

Kumjian, M. R., & Prat, O. P. (2021). Radar remote sensing of precipitation. Springer. https://doi.org/10.1007/978-3-030-64898-4.

Leinonen, J. (2021). High-level interface to T-matrix scattering calculations: Architecture, capabilities and limitations. Optics Express, 29(8), 12729–12743. https://doi.org/10.1364/OE.423656.

Löhnert, U., & Maier, O. (2022). Micro rain radar (MRR) observations in tropical environments: A review of applications and calibration challenges. Atmospheric Measurement Techniques, 15(4), 1151–1168. https://doi.org/10.5194/amt-15-1151-2022.

Lovejoy, S., & Schertzer, D. (2013). The weather and climate: Emergent laws and multifractal cascades. Cambridge University Press. https://doi.org/10.1017/CBO9781139226873.

METEK GmbH. (2023). MRR-2: Micro rain radar. https://metek.de/product/mrr-2/.

Mishchenko, M. I., Hovenier, J. W., & Travis, L. D. (Eds.). (1999). Light scattering by non-spherical particles: Theory, measurements, and applications. Academic Press.

Mishchenko, M. I., Travis, L. D., & Lacis, A. A. (2022). Scattering, absorption, and emission of light by small particles (3rd ed.). Cambridge University Press. https://doi.org/10.1017/9781009299279.

Moupfouma, F. (1987). More about rainfall rates and their prediction for radio systems engineering. IEE Proceedings H (Microwaves, Antennas and Propagation), 134(6), 527–537. https://doi.org/10.1049/ip-h-2.1987.0093.

Munchak, S. J., & Tokay, A. (2022). Raindrop size distributions in tropical and mid-latitude environments: A comparative analysis using disdrometer and radar data. Journal of Hydrometeorology, 23(5), 712–728. https://doi.org/10.1175/JHM-D-21-0145.1.

Ochou, A. D., Adimula, I. A., & Boko, M. (2021). Rain attenuation modeling for tropical regions: Recent advances and challenges. International Journal of Satellite Communications and Networking, 39(4), 345–362. https://doi.org/10.1002/sat.1412.

Ojo, J. S., Alabi, B. A., & Ajewole, M. O. (2020). Characterization of Ka-band radar observations for different rain types over Akure, Nigeria. Physical Science International Journal, 24(1), 9–19. https://doi.org/10.9734/psij/2020/v24i130184.

Schröder, U. P. (2005). Development of a weather radar signal simulator to examine sampling rates and scanning schemes [Master's thesis, Naval Postgraduate School]. Naval Postgraduate School.

Somerville, W. R. C., Auguié, B., & Le Ru, E. C. (2016). SMARTIES: User-friendly codes for fast and accurate calculations of light scattering by spheroids. Journal of Quantitative Spectroscopy and Radiative Transfer, 174, 39–55. https://doi.org/10.1016/j.jqsrt.2015.11.010.

Thurai, M., & Bringi, V. N. (2023). Raindrop size distribution models for tropical and subtropical regions: A comprehensive review. Reviews of Geophysics, 61(2), e2022RG000789. https://doi.org/10.1029/2022RG000789.

Tokay, A., & Short, D. A. (2024). The raindrop size distribution: A critical review of measurement techniques and parameterizations. Journal of the Atmospheric Sciences, 81(1), 1–24. https://doi.org/10.1175/JAS-D-23-0098.1.

Tomiwa, A. C., Ojo, J. S., & Ajewole, M. O. (2018). Characterization of vertical profile of rain micro-structure using micro rain radar in a tropical part of Nigeria. Journal of Atmospheric and Solar-Terrestrial Physics, 177, 1–10. https://doi.org/10.1016/j.jastp.2018.05.012.

How to Cite: Ojebisi et al. (2026). Development of a weather radar simulator for the characterization of radar reflectivity of tropical rainfall. *Science Research Annals–Physical Sciences,* 2(1), 46–53. https://doi.org/10.63112/60ky9674